

## Nanoarrays of Single Virus Particles\*\*

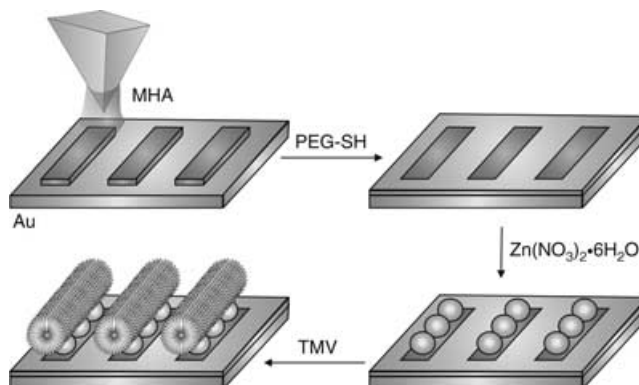
Rafael A. Vega, Daniel Maspoch, Khalid Salaita, and  
Chad A. Mirkin\*

Microarray technology has led to significant advances in many areas of medical and biological research,<sup>[1]</sup> opening up avenues for the combinatorial screening and identification of single-nucleotide polymorphisms (SNPs),<sup>[2]</sup> high-sensitivity expression profiling of proteins,<sup>[3,4]</sup> and high-throughput analysis of protein function.<sup>[5]</sup> With the advent of high-resolution direct-write lithographic methods such as dip-pen nanolithography (DPN),<sup>[6]</sup> it is possible to conceive of methods for miniaturizing such structures to the nanometer-length scale.<sup>[7–9]</sup> Such massive miniaturization provides the clear potential advantages of larger, denser libraries for screening complex chemical and biological systems. However, miniaturization on this size scale also provides the potential to site-isolate nano- and microscale biological entities (proteins, viruses, and cells) at the single-particle level. Once this can be done routinely for many different systems, new opportunities will be available to the biochemical and biomedical research communities to study such entities individually rather than collectively. Herein, we describe a novel strategy that uses DPN in combination with coordination chemistry to precisely immobilize and position many individual virus particles in the context of large arrays. Tobacco mosaic virus (TMV) was chosen as the test case scenario because of its anisotropic tubular structure (length  $\approx 300$  nm, diameter = 18 nm), size, stability, and well-characterized carboxylate-rich surface.<sup>[10]</sup> It serves as an excellent model system to evaluate how DPN can be used to control the positioning and orientation of nano-scale virus particles within an extended array.

Prior to this study, advances were made in immobilizing virus particles on templates created by DPN and  $\mu$ -contact printing.<sup>[11,12]</sup> Thus far, there has been no demonstration of the ability to chemically control the position of the immobilized virus structures at the single-particle level. This is partially the result of limited resolution, the size of the particles interrogated, and the chemistry used to immobilize them. Indeed, previous efforts focused on the genetic modification of a virus particle to present unnatural surface binding functionality to

the patterned interface.<sup>[11,12]</sup> This strategy has allowed researchers to prepare arrays of collections of virus particles at individual feature sites, but not to site-isolate individual particles. The approach used herein relies on the ability of metal ions ( $\text{Zn}^{2+}$ ) to bridge a surface patterned with features made of 16-thiohexadecanoic acid (MHA) and the TMV with its carboxylate-rich surface.

Virus nanoarrays were fabricated by initially generating chemical templates of MHA on a gold thin film by using DPN (Scheme 1). The regions surrounding these features were



**Scheme 1.** Selective immobilization of single virus particles on DPN-generated MHA nanotemplates treated with  $\text{Zn}(\text{NO}_3)_2 \cdot 6\text{H}_2\text{O}$ .

passivated with a monolayer of 11-thioundecyl-penta(ethylene glycol) (PEG-SH) by immersing the substrate in an alkanethiol solution (5 mM in ethanol) for 30 min followed by copious rinsing with ethanol. The passivation layer minimizes nonspecific binding of the virus particles to the unpatterned areas. The carboxylic acid groups of MHA were coordinated to  $\text{Zn}^{2+}$  ions (represented as spheres) by exposing the substrate to a solution of  $\text{Zn}(\text{NO}_3)_2 \cdot 6\text{H}_2\text{O}$  (5 mM in ethanol) for one hour followed by rinsing with ethanol to remove any unbound metal ions from the surface. The metallated substrate was then exposed to TMV ( $100 \mu\text{g mL}^{-1}$ , American Type Culture Collections) in phosphate-buffered saline (PBS, 10 mM with NaCl (0.15 M), pH 7) for 24 h at room temperature in an air-tight humidity chamber. Excess virus particles were removed by washing the substrates with highly purified (NANOpure) water. The cleaned substrates were then dried under a stream of  $\text{N}_2$ . All virus arrays were characterized by tapping mode AFM (TMAFM), and the chemical identity of the surface-immobilized virus particles was confirmed by treatment with a highly specific antiserum (American Type Culture Collections) against TMV, which upon binding increases the height of each virus particle (see below).

A series of DPN-patterned linear nanostructures of MHA with varied dimensions (length  $\times$  width:  $600 \times 200 \text{ nm}^2$ ,  $500 \times 180 \text{ nm}^2$ ,  $400 \times 50 \text{ nm}^2$ , and  $350 \times 110 \text{ nm}^2$ ) were systematically studied to determine the optimal feature size for single virus particle attachment. Under the conditions studied, MHA templates with feature dimensions of  $350 \times 110 \text{ nm}^2$  spaced one micrometer apart were ideal for individual particle assembly. The tendency of each virus to occupy the largest number of coordination sites results in near-perfect alignment

[\*] R. A. Vega, Dr. D. Maspoch, K. Salaita, Prof. C. A. Mirkin  
Department of Chemistry and Institute for Nanotechnology  
Northwestern University  
2145 Sheridan Road, Evanston, IL 60208-3113 (USA)  
Fax: (+1) 847-467-5123  
E-mail: chadnano@northwestern.edu

[\*\*] C.A.M. acknowledges the AFOSR, ARO, DARPA, NIH, and NSF for support of this work. R.A.V. thanks the NIH for predoctoral support, and D.M. is grateful to the Generalitat de Catalunya for a postdoctoral grant.

Supporting information for this article is available on the WWW under <http://www.angewandte.org> or from the author.

of all the virus particles along the long axis of each rectangular template (Figure 1 a,b). The average height of each feature on the template is  $16 \pm 1$  nm. Furthermore, each virus particle on the lines is  $45 \pm 2$  nm wide and  $320 \pm 40$  nm long (measured at the base, disregarding tip convolution), parameters consistent

particle was tested by immobilization along two different directions within one array. Indeed, the use of an MHA template consisting of  $350 \times 110$  nm<sup>2</sup> features perpendicular to each other produced an array of site-isolated single TMV virus particles perpendicular to each other (Figure 1 b).

Polarization modulation infrared reflection absorption spectroscopy (PM-IRRAS) was used to characterize bulk gold thin-film substrates modified with TMV by using the same coordination chemistry approach used to generate the TMV arrays (Figure 2 a). The MHA monolayer exhibits two main bands in the high-frequency CH<sub>2</sub> stretch region at 2856 and 2930 cm<sup>-1</sup> and two in the C=O stretch region at 1741 and 1718 cm<sup>-1</sup>, which are attributed to the presence of free and hydrogen-bonded carboxylic groups,<sup>[15]</sup> respectively. After the substrate was immersed in an ethanolic solution of Zn(NO<sub>3</sub>)<sub>2</sub>·6H<sub>2</sub>O (5 mM) for 1 h, the coordination of MHA carboxylic groups to Zn<sup>2+</sup> metal ions was confirmed by  $\Delta_{\text{CO}}$  band shifts to lower energy ( $\tilde{\nu} = 1602/1556$  and 1453 cm<sup>-1</sup>). The C=O stretch region changes again after exposing the MHA–Zn<sup>2+</sup> surface to the TMV solution. Three main bands are detected in this spectral region that can be identified as the amide I band centered at 1661 cm<sup>-1</sup> (which is characteristic of proteins in TMV<sup>[16]</sup>), the amide II and asymmetric COO<sup>-</sup> bands centered at 1546 cm<sup>-1</sup>, and a symmetric COO<sup>-</sup> band at 1458 cm<sup>-1</sup>. Also, the presence of CH<sub>3</sub> features,

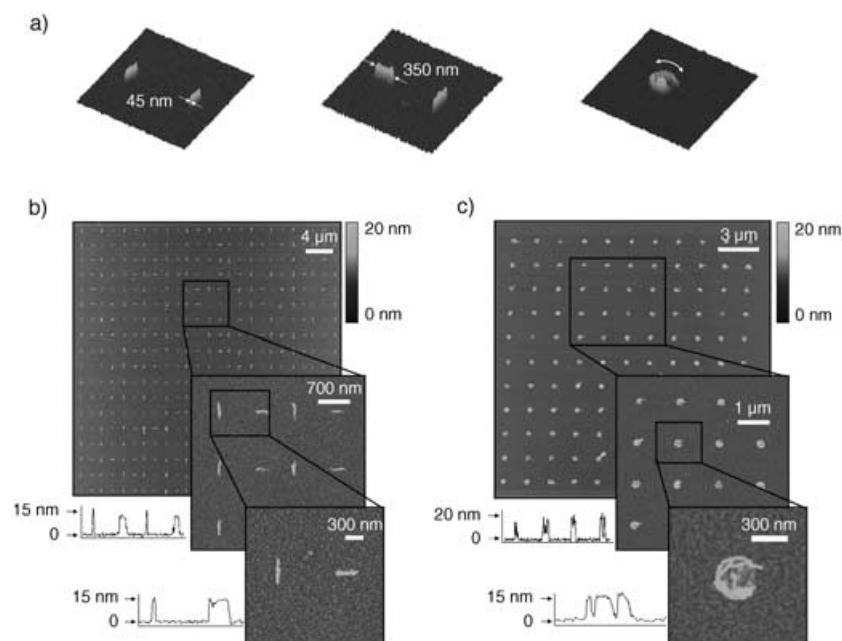


**Figure 1.** AFM tapping mode (silicon cantilever, spring constant  $\approx 40$  N m<sup>-1</sup>) images and height profiles of TMV nanoarrays: a) 3D topographical images of pairs of virus particles within larger arrays: a parallel array (left), a perpendicular array (middle), and dot arrays (right); b) topography images and height profiles of a perpendicular array of single virus particles ( $40 \times 40$  μm<sup>2</sup>); c) topography image and height profiles of a TMV nanoarray ( $20 \times 20$  μm<sup>2</sup>) formed on an array of MHA dot features ( $\varnothing = 350$  nm) pretreated with Zn(NO<sub>3</sub>)<sub>2</sub>·6H<sub>2</sub>O. All images were collected at a scan rate of 0.5 Hz.

with the presence of only one TMV particle on each MHA feature.<sup>[13]</sup> The dimensions of the features within the array are critical for virus particle site-isolation. For example, rectangular templates greater than 500 nm long or 200 nm wide yield multiple yet oriented viruses at each site, thus preventing the formation of a single virus particle array (see Supporting Information). Features significantly smaller (less than  $300 \times 100$  nm<sup>2</sup>) do not result in uniform assembly of the virus particles; numerous sites remain unoccupied.

The chemical templates can also be used to control the assembly of the flexible virus into unnatural conformations such as circles and other curved architectures. For example, dot templates 350 nm in diameter can capture multiple virus particles, many of which adhere to the rim of the dot and adopt a curved shape (Figure 1 c). Curved TMV structures have been made previously, but through mechanical manipulation of the virus.<sup>[14]</sup> This approach to virus bending is different from the templated chemical approach described herein.

To demonstrate that the virus orientation is not the result of external variables such as washing, drying with N<sub>2</sub>, or capillary effects, the independent organization of each virus

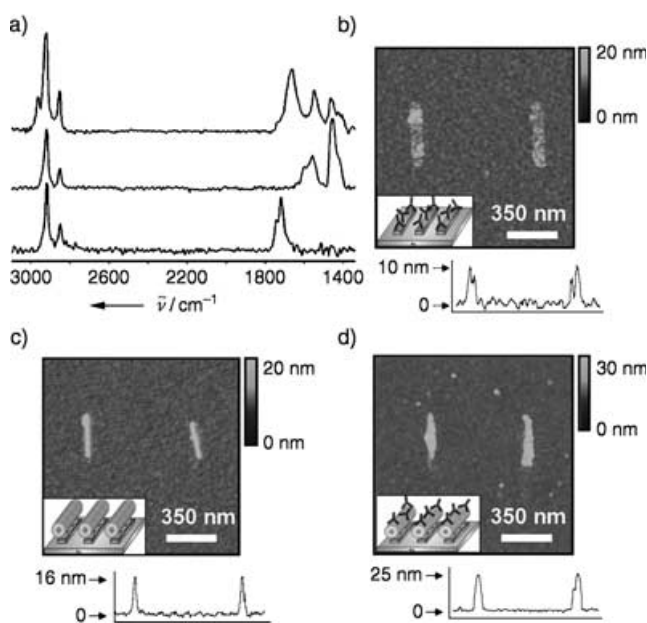


**Figure 2.** a) PM-IRRAS spectra of a monolayer of MHA on Au (bottom spectrum), after treatment with Zn(NO<sub>3</sub>)<sub>2</sub>·6H<sub>2</sub>O (middle spectrum), and subsequent incubation with TMV (top spectrum). b) Topography image and height profile of an MHA array treated with the antiserum against TMV. The antibodies are electrostatically attached to the MHA features. Topography images and height profiles of a pair of parallel single virus particles c) before and d) after treatment with a PBS solution containing the antiserum against TMV. All AFM images were taken at a scan rate of 0.5 Hz in tapping mode.

attributed to proteins with methyl groups, is confirmed by the emergence of a new band at  $2967\text{ cm}^{-1}$  after incubation with TMV.

The coordination chemistry of  $\text{Zn}^{2+}$  is essential for the virus particle assembly process. The results of control experiments support this conclusion, as TMV does not assemble on MHA coated or patterned substrates (dot diameter =  $1\text{ }\mu\text{m}$ ), even after exposure of the template to the virus in a PBS solution for 48 h.

To provide further evidence for the chemical identity of the tubular virus structures imaged by AFM, the single virus arrays were treated with a PBS solution containing an antiserum against TMV ( $200\text{ }\mu\text{g mL}^{-1}$ , pH 7) at  $37^\circ\text{C}$  for 30 minutes. The substrates were rinsed with PBS and then dried under a stream of  $\text{N}_2$ . A comparison of the AFM images of the substrate before and after incubation with antibody shows a height increase of approximately 9 nm (Figure 2c,d). This increase is consistent with the height of the antibody (Figure 2b) and therefore, the presence of TMV particles on the arrays.<sup>[17]</sup> Note that the expected height increase upon antibody binding was independently modeled and measured by using direct adsorption of the antibody onto an MHA array (Figure 2b). This approach has been used to study protein binding events in the context of other protein immobilization experiments.<sup>[8]</sup>

In conclusion, we report a versatile coordination-chemistry-based approach for the immobilization of TMV virus particles on surfaces and show that through the use of DPN and small features, it is possible to isolate and control the orientation of these virus particles. Many virus particles have metal-binding groups for  $\text{Zn}^{2+}$  and other ions in their protein coats.<sup>[18]</sup> Therefore, it is likely that this approach can be generalized for manipulating many virus structure classes at the single-particle level. Such capabilities will expand the scope of application for virus structures in fields ranging from biology to molecular electronics,<sup>[19]</sup> in which such control opens new opportunities for research that cannot be addressed with microarrays or bulk systems.

## Experimental Section

All DPN patterning was done with a CP AFM (ThermoMicroscopes) interfaced with commercialized lithographic software (DPNwrite, NanoInk Inc., Chicago, IL) and conventional  $\text{Si}_3\text{N}_4$  cantilevers (ThermoMicroscopes-sharpened Microcantilever A, force constant =  $0.05\text{ N m}^{-1}$ ). Tapping mode images were taken with a Nano-scope IIIa and MultiMode microscope (Digital Instruments). Unless noted otherwise, all DPN patterning experiments were conducted at 35 % relative humidity and  $24^\circ\text{C}$  with a tip–substrate contact force of 0.5 nN. DPN was used to pattern MHA on gold substrate (50 nm Au and 10 nm Cr on a silicon wafer, Silicon Sense, Inc.). PM-IRRAS spectra of 2048 scans at a resolution of  $4\text{ cm}^{-1}$  were obtained with a Thermo Nicolet Nexus 870 with tabletop optics module (TOM) (courtesy of the Keck II Center at Northwestern University). The PM-IRRAS differential reflectance ( $\%\Delta R/R$ ) values were converted into absorbance units for comparison with conventional IRRAS data.

Received: June 7, 2005

Published online: August 22, 2005

**Keywords:** coordination modes · nanotechnology · scanning probe microscopy · surface chemistry · viruses

- [1] U. R. Miller, D. V. Nicolau, *Microarray Technology and Its Applications*, Springer, New York, **2005**.
- [2] K. Lindroos, S. Sigurdsson, K. Johansson, L. Ronnblom, A. C. Syvanen, *Nucleic Acid Res.* **2002**, *30*, e70–e78.
- [3] M. Schena, D. Shalon, R. W. Davis, P. O. Brown, *Science* **1995**, *270*, 467–470.
- [4] R. A. Heller, M. Schena, A. Chai, D. Shalon, T. Bedilion, J. Gilmore, D. E. Woolley, R. W. Davis, *Proc. Natl. Acad. Sci. USA* **1997**, *94*, 2150–2155.
- [5] G. MacBeath, S. L. Schreiber, *Science* **2000**, *289*, 1760–1763.
- [6] a) D. S. Ginger, H. Zhang, C. A. Mirkin, *Angew. Chem.* **2004**, *116*, 30–46; *Angew. Chem. Int. Ed.* **2004**, *43*, 30–45; b) R. D. Piner, J. Zhu, F. Xu, S. Hong, C. A. Mirkin, *Science* **1999**, *283*, 661–663.
- [7] For an example of DNA nanoarrays, see: L. M. Demers, D. S. Ginger, S.-J. Park, Z. Li, S.-W. Chung, C. A. Mirkin, *Science* **2002**, *296*, 1836–1838.
- [8] For an example of protein nanoarrays, see: a) K.-B. Lee, S.-J. Park, C. A. Mirkin, J. C. Smith, M. Mrksich, *Science* **2002**, *295*, 1702–1705; b) K.-B. Lee, J.-H. Lim, C. A. Mirkin, *J. Am. Chem. Soc.* **2003**, *125*, 5588–5589; c) J.-H. Lim, D. Ginger, K.-B. Lee, J. Heo, J.-M. Nam, C. A. Mirkin, *Angew. Chem.* **2003**, *115*, 2411–2414; *Angew. Chem. Int. Ed.* **2003**, *42*, 2309–2312.
- [9] For an example of peptide nanoarrays, see: J. Hyun, W. K. Lee, N. Nath, A. Chilkoti, S. Zauscher, *J. Am. Chem. Soc.* **2004**, *126*, 7330–7335.
- [10] a) T. M. A. Wilson, R. N. Perham, *Virology* **1985**, *140*, 21–27; b) L. King, R. Leberman, *Biochim. Biophys. Acta* **1973**, *322*, 279–293.
- [11] C. L. Cheung, J. A. Carnarero, B. W. Woods, T. Lin, J. E. Johnson, J. J. Yoreo, *J. Am. Chem. Soc.* **2003**, *125*, 6848–6849.
- [12] J. C. Smith, K.-B. Lee, Q. Wang, M. G. Finn, J. E. Johnson, M. Mrksich, C. A. Mirkin, *Nano Lett.* **2003**, *3*, 883–886.
- [13] a) M. Knez, M. P. Sumser, A. M. Bittner, C. Wege, H. Jeske, D. M. P. Hoffmann, D. M. P. Kuhnke, K. Kern, *Langmuir* **2004**, *20*, 441–447; b) H. Maeda, *Langmuir* **1997**, *13*, 4150–4161, and references therein.
- [14] M. Guthold, M. Falvo, W. G. Matthews, S. Paulson, J. Mullin, S. Lord, D. Erie, S. Washburn, R. Superfine, F. P. Brooks Jr., R. M. Taylor II, *J. Mol. Graphics Modell.* **1999**, *17*, 187–197.
- [15] B. L. Frey, R. M. Corn, *Anal. Chem.* **1996**, *68*, 3187–3193.
- [16] R. D. B. Fraser, *Nature* **1952**, *170*, 491.
- [17] Antibody arrays were generated by first using DPN to pattern rectangular lines of MHA with feature dimensions of  $350 \times 110\text{ nm}^2$ . The area around these features was passivated with PEG-SH for 30 min, followed by copious rinsing with ethanol to inhibit nonspecific binding. Finally, the antiserum against TMV was incubated with the MHA-passivated substrate at  $4^\circ\text{C}$  for 24 h. For more details, see reference [8].
- [18] a) A. Nedoluzhko, T. Douglas, *J. Inorg. Biochem.* **2001**, *84*, 233–240; b) G. Basu, M. Allen, D. Willits, M. Young, T. Douglas, *J. Biol. Inorg. Chem.* **2003**, *8*, 721–725.
- [19] a) W. Shenton, T. Douglas, M. Young, G. Stubbs, S. Mann, *Adv. Mater.* **1999**, *11*, 253–256; b) E. Dujardin, C. Peet, G. Stubbs, J. M. Culver, S. Mann, *Nano Lett.* **2003**, *3*, 413–417; c) M. Knez, A. M. Bittner, F. Boes, C. Wege, H. Jeske, E. Mai, K. Kern, *Nano Lett.* **2003**, *3*, 1079–1082.